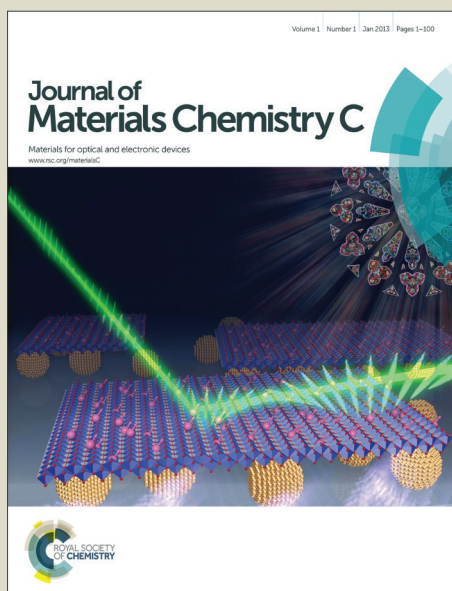


# Journal of Materials Chemistry C

Accepted Manuscript



This is an *Accepted Manuscript*, which has been through the Royal Society of Chemistry peer review process and has been accepted for publication.

*Accepted Manuscripts* are published online shortly after acceptance, before technical editing, formatting and proof reading. Using this free service, authors can make their results available to the community, in citable form, before we publish the edited article. We will replace this *Accepted Manuscript* with the edited and formatted *Advance Article* as soon as it is available.

You can find more information about *Accepted Manuscripts* in the [Information for Authors](#).

Please note that technical editing may introduce minor changes to the text and/or graphics, which may alter content. The journal's standard [Terms & Conditions](#) and the [Ethical guidelines](#) still apply. In no event shall the Royal Society of Chemistry be held responsible for any errors or omissions in this *Accepted Manuscript* or any consequences arising from the use of any information it contains.



Journal Name

COMMUNICATION

## Brush-Controlled Oriented Growth of TCNQ Microwire Arrays for Field-Effect Transistors

Received 00th January 20xx,  
Accepted 00th January 20xx

Peng Zhang, Qingxin Tang,\* Yanhong Tong, Xiaoli Zhao, Guorui Wang, and Yichun Liu\*

DOI: 10.1039/x0xx00000x

www.rsc.org/

**We demonstrate a novel solution-based assembly method by a writing brush to realize the controllable fabrication of highly-oriented and large-scale TCNQ single-crystal microwire arrays. The arrays can be grown not only on the conventional rigid substrates such as Si, Si/SiO<sub>2</sub> and low-cost glass, but also on the nonconventional substrates which include the flexible polyethylene terephthalate (PET), the curved glass hemisphere, and commercially available plastic contact lens. Its morphology is optimized by solution concentration, substrate temperature, brush type, inclination angles and pressure of the brush. The length of the microwire arrays can extend up to the millimeter level, and their preferential orientation is controlled perpendicular to the location direction of the brush hair. The coverage area of the microwire arrays with the consistent orientation can reach as large as 1.5×2.0 mm<sup>2</sup>, and the success ratio is as high as 93%. Based on these microwire arrays, the devices on different substrates including rigid Si/SiO<sub>2</sub> and flexible PET can be easily realized in one step. The anisotropic transport of TCNQ crystals is studied based on the concentration controlled morphology. All these results illustrate the broad application prospect of this facile brush writing method in the growth of the large-scale high-quality organic micro/nanowires and integration of flexible organic semiconductor devices and circuits.**

### Introduction

Solution-processed oriented growth of organic single-crystal micro/nanowire arrays offers great potential for achieving low-cost and large-scale production for flexible electronics.<sup>1-2</sup> A traditional method is to dissolve an organic material into a volatilizable organic solvent, and then simply drop the solution onto a target substrate.<sup>3-4</sup>

The solvent evaporation induced droplet shrinking competes with the contact line pinning coming from the solution/substrate interface interaction, leading to the precipitation of organic crystals in the direction of solvent evaporation.<sup>5</sup> This method is easily realized but is sensitive to environment, and therefore shows low reliability and controllability. Controlled alignment of organic single-crystal micro/nanowires requires the new designed methods. Thus, most of the current researches have been focusing on how to develop methods for the improvement of orientation, dimension, crystalline quality, success ratio, coverage area, and precise location.<sup>6-13</sup> Recently, a new use of micropillar-patterned shearing blades has been demonstrated to improve the morphology of TIPS-pentacene single-crystal arrays with remarkably reduced grain boundary densities and eliminated dendritic domain.<sup>14</sup> Another amazing method, high-speed electrohydrodynamic print technique, has been reported to enable the growth of the highly aligned, individual controlled organic single-crystal nanowire at desired positions.<sup>15</sup> Currently, most reported solution-processed organic single-crystal micro/nanowire arrays focus on p-channel materials.<sup>3,4,16-19</sup> The lack of the n-channel organic materials brings one crucial challenge for future electronic applications in the most extensively used CMOS circuits.<sup>20</sup>

TCNQ is a typical n-type organic small molecule semiconductor material, with the band gap of 2.25 eV and the LUMO energy level of 4.6 eV. It belongs to the monoclinic crystal system *C2/c* and has the lattice parameters of *a*=8.906 Å, *b*=7.060 Å, *c*=16.395 Å, and  $\beta$ =98.65°. <sup>21</sup> The parallel and staggered arrangement mode between the molecules causes the effective molecular overlap for improved carrier mobility.<sup>22</sup> The individual TCNQ micro/nanowire is easily precipitated from a solution evaporation process which has been addressed by a few research groups. In contrast, the reports on growth of TCNQ micro/nanowire arrays are very limited. Until now, only Biswanath Mukherjee's group has reported the growth of the oriented TCNQ arrays by a capillary assistant method.<sup>23</sup> However, this method is not preferred in the case of TCNQ because it leads to undesired morphology with dendritic growth that holds back

Key Laboratory of UV-Emitting Materials and Technology (Northeast Normal University), Ministry of Education, Changchun 130024, P. R. China. \*E-mail: tangqx@nenu.edu.cn

efficient carrier transport due to charge trapping at the prevalent grain boundaries.

In this paper, we developed a novel solution-based assembly method based on a writing brush to yield highly-oriented, well-separated and single-crystal TCNQ microwire arrays at high success ratio and at large scale. The brush hair induces the capillary force to change the flowing direction of the solution, causing a smaller solution concentration gradient and hence a larger-area single-crystal microwire arrays. The TCNQ microwire arrays tightly adhere on the substrate surface with a length extending up to millimeter level. And they are single crystals with the preferential orientation perpendicular to the location direction of the brush hair. The coverage area of the microwire arrays with the consistent orientation can reach as large as  $1.5 \times 2.0 \text{ mm}^2$ . The success ratio of microwire arrays achieved by this method is as high as 93%. Based on the large-area single-crystal TCNQ microwire arrays, we fabricated the field effect transistors on rigid and flexible substrates, which show the typical n-type characteristic in the air at room temperature. All these results illustrate the broad application prospect of this facile brush writing method on the growth of the high-quality organic micro/nanowires, large-scale integration of the flexible organic semiconductor devices and circuits.

## Experimental section

### Growth of microwire arrays and microsheets

Based on a writing brush (wolf hair, wolf/goat hair, and goat hair), TCNQ microwire arrays and microsheets were obtained by the solution-processed assembly method on a wide variety of substrates (Si, Si/SiO<sub>2</sub>, glass, and polyethylene terephthalate (PET), curved glass hemisphere, and even commercially available plastic contact lens). The inorganic substrates (Si, Si/SiO<sub>2</sub>, glass and glass hemisphere) were cleaned by sonication in acetone for 15 min and dried on a filter paper. Then these substrates were immersed in the chromic acid lotion for 10 min, followed by cleaning with flowing deionized water and drying in the ordinary nitrogen atmosphere. After that, substrates were treated with oxygen plasma for 2 min. For the flexible PET substrate, it was just cleaned with acetone and ethanol for 10 min, then dried with nitrogen gas and treated with oxygen plasma before use. For the plastic contact lens, it was directly cleaned with contact lens solution, then dried in air and treated with oxygen plasma before use. TCNQ powders (Aldrich, 98%) were purified by sublimation in a flowing nitrogen gas atmosphere under the low pressure at 140 °C. Purified TCNQ was dissolved in acetonitrile (Sigma-Aldrich,  $\geq 99.93\%$ ) at a concentration of 0.2-3 g/L. The growth of the microwire arrays and microsheets were carried out at different substrate temperatures under atmospheric conditions. The microwires and microsheets were fabricated by immersing the writing brush into the CH<sub>3</sub>CN solution of TCNQ, and pressing it on the substrate, and then putting it up. When the solution concentration was lower than 2.5 g/L, the TCNQ

microwire arrays were obtained. When the solution concentration ranged from 2.5 to 3 g/L, TCNQ microsheets were achieved with the lateral dimension of 20 -60  $\mu\text{m}$ .

### Device fabrication

#### Bottom-gate bottom-contact configuration devices

The devices were fabricated in bottom-gate bottom-contact geometry based on TCNQ microwire arrays and microsheets using OTS-modified Si/SiO<sub>2</sub> substrates and SiO<sub>2</sub> dielectrics. The thickness of SiO<sub>2</sub> layer was 300 nm. Dielectric capacitance is generally  $\sim 1 \times 10^{-8} \text{ Fcm}^{-2}$ . First, Au electrodes were patterned on the Si/SiO<sub>2</sub>/OTS and Si/SiO<sub>2</sub> substrate using photolithography with a shadow mask and an electrode deposition process. Then, TCNQ microwire arrays and microsheets were obtained using TCNQ/ CH<sub>3</sub>CN solution at concentration of 0.8 g/L and 2.5 g/L with the substrate temperature of 70 °C. In the growth process of TCNQ microwire arrays and microsheets, the microwire arrays and microsheets were connected with the micro-fabricated electrodes.

#### Bottom-gate top-contact configuration devices

Based on TCNQ microwire arrays, the flexible devices in bottom-gate top-contact configurations were fabricated on PET substrate using Poly(vinyl alcohol) (PVA) (Aldrich, average Mw  $\sim 205,000 \text{ g/mol}$ ) as dielectric by the "gold film stamping" method.<sup>24</sup> First, the 100  $\mu\text{m}$ -thick PET sheet was used as supporting layer and PVA was used as dielectric. 50 nm-thick Au was evaporated on the PET as the gate electrode. PVA was dissolved in deionized water and deposited on the Au film as the dielectric layer by spin coating. The thickness of PVA insulation layer was  $\sim 83 \text{ nm}$ . Dielectric capacitance is generally  $\sim 1 \times 10^{-8} \text{ Fcm}^{-2}$ . Then, TCNQ microwire arrays were fabricated on that using TCNQ/ CH<sub>3</sub>CN solution at concentration of 0.8 g/L with the substrate temperature of 70 °C. Finally the thin Au layers (100 nm) were stamped onto TCNQ microwire arrays as the source/drain electrodes owing to its high tenacity and good tractility.

### Characterization

Optical microscopy images were obtained by an Olympus BX51. Structural properties were characterized by out-of-plane XRD pattern from a D8 discovery thin-film diffractometer with Cu K $\alpha$  radiation (1.54056 Å) with voltage at 40 kV and current at 35 mA. Scanning electron microscope (SEM) images were obtained by the Micro FEI Philips XL-30 ESEM FEG. Atomic force microscopy (AFM) measurements were carried out on a Bruker Dimension Icon instrument. The electrical properties of TCNQ devices were recorded with a Keithley 4200-SCS and a Cascade M150 probe station in a clean and shielded box at room temperature in air. All OFET measurements were performed in air and the mobility was extracted in the saturation regime in this work.

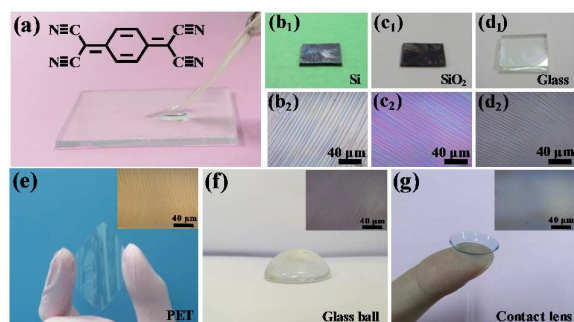


**Fig. 1** (a) Digital photograph of the brush writing method to grow TCNQ microwire arrays on the glass substrate. The inset shows the molecular structure of TCNQ. (b<sub>1</sub>-d<sub>1</sub>) The TCNQ microwire arrays can grow on Si, Si/SiO<sub>2</sub> and low-cost glass substrate. (b<sub>2</sub>-d<sub>2</sub>) The corresponding optical microscope images. (e-g) The TCNQ microwire arrays can grow on flexible PET, curved glass hemisphere, and even commercially available plastic contact lens substrate. The insets are corresponding optical microscope images.

## Results and discussion

We presented a novel solution-based assembly method to realize the oriented growth of TCNQ microwire arrays by a writing brush. Firstly, the writing brush was immersed into the pre-prepared solution to store enough solution for the growth of TCNQ microwire arrays. And then, it was pressed onto a target substrate resulting in the outward spread of the solution. Finally, the writing brush was put up slowly, the large-area and ordered microwire arrays could be formed with the solvent evaporation. Fig. 1a shows a writing brush pressed onto a typical substrate, and the inset is the molecular structure of TCNQ. To examine the ability of this method to be compatible to various final destination substrates, we brush the solution to different objects which can be rigid or flexible, organic or inorganic, planar or curved. Fig. 1b-g show the TCNQ microwire arrays can be grown on Si, Si/SiO<sub>2</sub>, low-cost glass, flexible PET, curved glass hemisphere, and even commercially available plastic contact lens. These results illustrate the promising potential of TCNQ microwire arrays for next-generation flexible and wearable electronics.

The typical morphology features of TCNQ microwire arrays are shown in Fig. 2a-d. When the solution concentration is lower than 2.5 g/L, the large scale, highly ordered microwire arrays with good dispersity can be formed. They show the preferential orientation approximately perpendicular to the location direction of the brush hair. These microwires tightly adhere on the substrate surface with a length extending up to millimeter level. Their width can change from 0.5 to 2 μm. The individual crystal shows the uniform color and brightness between crossed polarizers under the observation of the optical microscope images (Fig. 2d<sub>1</sub>-d<sub>4</sub>), confirming the anisotropic crystalline nature of the oriented microwire arrays.<sup>5</sup> The SEM results show that the TCNQ microwires are regular shapes and smooth

edges (see Supporting Information). The coverage area of the microwire arrays with the consistent orientation can reach as large as 1.5×2.0 mm<sup>2</sup>. The out-of-plane XRD pattern only shows a sharp diffraction peak, which confirms the preferred orientation and high quality of microwire arrays (see Supporting Information). Further, we evaluated the yield of microwire arrays grown in the same alignment direction from 40 samples on 0.6×0.6 cm<sup>2</sup> Si substrates. As shown in Fig. 2e, the yield at area over 1.0×1.5 mm<sup>2</sup> reaches 18%, and the yield at area over 0.5×1.0 mm<sup>2</sup> is as high as 60%. We also explored the potential of this method for practical application, by evaluating the success ratio from 80 samples. As shown in Fig. 2f, the success ratio of microwire arrays achieved by this method is 93%, which is far higher than that achieved in a conventional drop-casting method (50%). To assess the coverage degree of this method, the location of the microwire formation is labeled in Fig. 3a, and the results were compared with that of a conventional drop-casting method. Fig. 3b<sub>1</sub>-b<sub>4</sub> is the optical microscope images of a typical sample at the different regions, which respectively correspond to the locations labeled as b<sub>1</sub>-b<sub>4</sub> in Fig. 3a. Using our brush-controlled method, the coverage of the highly ordered crystals on the 1×0.6 cm<sup>2</sup> Si substrate is over 94.8%. In contrast, a conventional drop-casting method produces the microwire arrays with polycrystalline domains and dendritic morphology, as shown in Fig. 3c-d. And the microwire arrays are only located at the edges of the substrate with a low coverage. Our method therefore shows outstanding advantages for the growth of TCNQ microwire arrays in improved crystalline quality, orientation, success ratio, yield and coverage degree.

To obtain the optimized morphology of TCNQ microwires, the solution concentration was modulated. As shown in Fig. 4a, when the concentration is 0.2 g/L, the thin microwire arrays with dendritic edges is formed, which shows that the growth is related to diffusion limited aggregation (LDA) possibly coming from low concentration-induced mass transport.<sup>25, 14</sup> When the concentration is 1.4 g/L, the fast nucleation and growth speed cause the formation of polycrystalline microstructure arrays, as shown Fig. 4c. Only when the concentration is near 0.8g/L, the TCNQ single-crystal microwire arrays with uniform color and good alignment are generated as shown in Fig. 4b. Interesting, by increasing the concentration up to the near saturated solution (2.5 g/L), the large-scale regular and uni-

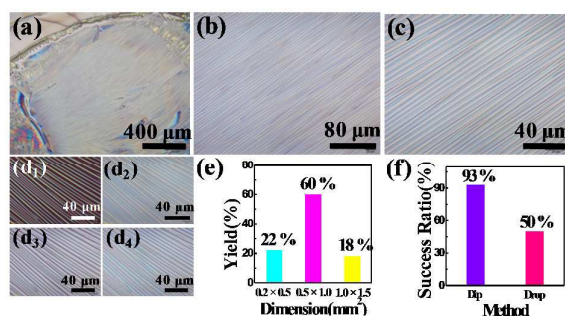


**Fig. 2** (a-c) Optical microscope images of TCNQ microwire arrays under different magnification, showing the large scale, highly order

and good dispersity. (d<sub>1</sub>-d<sub>4</sub>) Polarization optical microscope images under angles of (d<sub>1</sub>) 0° (d<sub>2</sub>) 30° (d<sub>3</sub>) 100° (d<sub>4</sub>) 140°, indicating the single-crystal nature of the oriented arrays. (e) The yields of microwire arrays vs dimensions from 40 samples on 0.6 × 0.6 cm<sup>2</sup> Si substrates. (f) Success ratios for the formation of TCNQ microwire arrays using brush-writing method and drop-casting method, respectively.

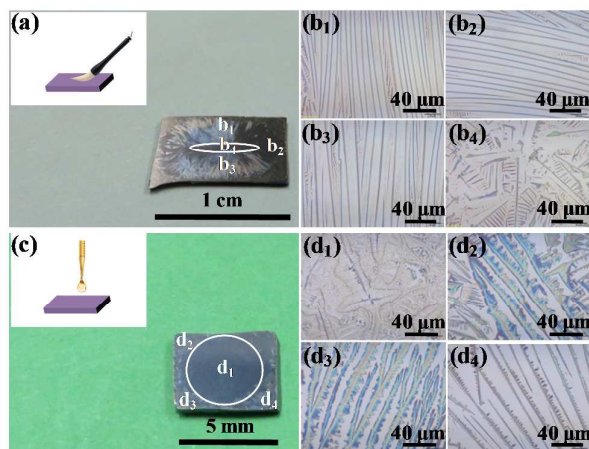


**Fig. 3** (a) Digital photograph of the sample by brush-writing method. The inset schematically shows the method. (b<sub>1</sub>-b<sub>4</sub>) Optical microscope images of TCNQ structures at different regions, which respectively correspond to the locations labeled as b<sub>1</sub>-b<sub>4</sub> in (a). (c) Digital photograph of the sample by drop-casting method. The inset schematically shows the method. (d<sub>1</sub>-d<sub>4</sub>) Optical microscope images of TCNQ structures at different regions, which respectively correspond to the locations labeled as d<sub>1</sub>-d<sub>4</sub> in (c).

form TCNQ microsheets with the size of 20-60 μm can be obtained with the brush-controlled solution process, as shown in Fig. 4d. The polarized optical microscope images exhibit homogeneous color for each microsheel under different polarization angles, indicating high crystalline quality of the formed TCNQ microsheets, as shown in Fig. 4e-h. In previous reports, the sheet-like TCNQ microcrystals were obtained mainly by a vapor transport method.<sup>26-27</sup> In contrast, the solution method possesses attractive advantages such as low cost, high reproducibility, high yield, and compatibility with large-scale production. Currently, Hui Jiang's group obtained the TCNQ microsheets with thickness at approximately 7 μm by the drop-casting method.<sup>22</sup> Jun Yang's group obtained the TCNQ nanosheets by a typical surfactant assisted solution method with over ten hours.<sup>28</sup> Here, we prepared highly-dispersed TCNQ microsheets which can be observed under the optical microscope. The AFM measurement results show that the thinnest sheets have the thickness at ~50-60 nm (see Supporting Information). Previous reports have addressed the dependence of the transport properties on the organic crystal thickness. For example, Tao et al. found that the mobility of the 4,4'-bis((E)-2-(naphthalen-2-yl)vinyl)-1,1'-biphenyl

(BNVBP) plates increased dramatically when the thickness was lower than 400 nm.<sup>30</sup> Our previous results have also shown that the carrier mobility increased from 6.4 × 10<sup>-3</sup> to 0.13 cm<sup>2</sup>V<sup>-1</sup>s<sup>-1</sup> with the decrease of the thickness in dinaphtho[3,4-d:3',4'-d']benzo[1,2-b:4,5-b']dithiophene (Ph5T2) crystal from 56 to 14 nm.<sup>29</sup> The thin crystal enables the formation of the tight contact with the dielectric, and decreases the parasitic resistance of the top-contact devices when the current flow across the crystal thickness.<sup>31</sup> Therefore, the thin crystal obtained in our experiments shows the potential for improved carrier transport.

It is critical to control their orientation with area as large as possible. The orientation change possibly leads to an unpredicted variation in device fabrication, resulting in the decreased device yield. Here we fixed the concentration at 0.8 g/L, and brushed the solution onto the substrates heated at the different temperatures, to obtain the optimized temperature for more highly ordered and larger scale alignment. Fig. 5a-d shows the optical microscope images of the TCNQ microwire arrays formed at the substrate temperature of 25, 40, 70, and 100 °C, respectively. The results show that the oriented alignment of the microwire arrays with the coverage area as large as 1.5 × 2.0 mm<sup>2</sup> could be obtained when the substrate temperature is at 70 °C, which shows the promising potential for one-step production of large-scale microwire devices.

In order to understand the influence of different parameters of the writing brush on the growth of microwire arrays, we investigate different inclination angles, pressures, and types of the writing brush, respectively at room temperature, as shown in Figure 6, Figure 7 and Figure 8. When the angle between the brush and the substrate is 0°, only a little solution wets on the substrate, resulting in small area of the solution spread. In this case, no continuous microwires were formed. When the angle is increased, more solution wets on the substrate. When the brush almost is perpendicular to the substrate, the solution can spread on the whole substrate resulting in the formation of large-area nanowire array. As shown in Figure 7, we investigated the effect of the pressure of the brush on the growth of microwires. The higher pressure facilitates more solution wetting and spreading on the substrate, resulting in the formation of larger-area nanowire array. As shown in Figure 8, we also study the effect of the type of the brush, which includes wolf-hair, wolf/goat-hair, goat-hair brushes. It is found that the wolf brush can bring more solution onto the target substrate, which facilitates the growth of large-area microwire array, as shown in Figure 8.

In order to gain insight into the spontaneous alignment of TCNQ microwires, we have investigated the dynamics process of the solution under the observation of the optical microscope. As shown in Fig. 9a, when the writing brush is pressed on the target substrate, the solution is brought to contact with the substrate surface. The pressure of the brush on the substrate helps spread the solution outwards. Next, the brush was gently put up, which brought the spread solution to flow towards the brush (Fig. 9b). Once the brush

was moved away, the solution spread outwards again (Fig. 9c) and then an evaporation process occurred for the formation of microwire

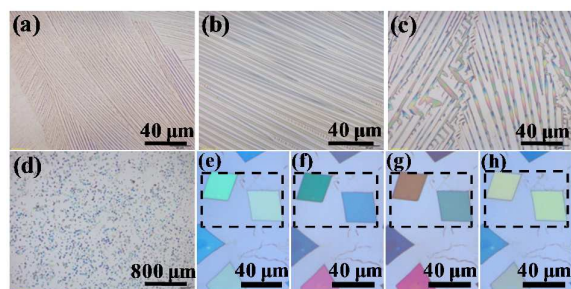


**Fig. 4** Optical microscope images of TCNQ arrays prepared from TCNQ solution in acetonitrile with different concentrations: (a) 0.2 (b) 0.8 (c) 1.4 and (d) 2.5 g/L. (e-h) Polarization optical microscope images of microsheets under angles of (e) 0° (f) 50° (g) 90° (h) 150°, indicating the single-crystal structure. The microsheets are obtained with the concentration of 2.5 g/L on the silicon substrate.

arrays (Fig. 9d-f). We believe that the brush hair induced capillary force changes the flowing direction of the solution, and brings a more ordered alignment of the microwires. The first outward spread of the solution induced by pressing the brush is possibly favorable for the wetting of the solution onto the substrate surface for the second outward spread, which causes a more smaller solute concentration gradient and hence a larger-area microwire array.

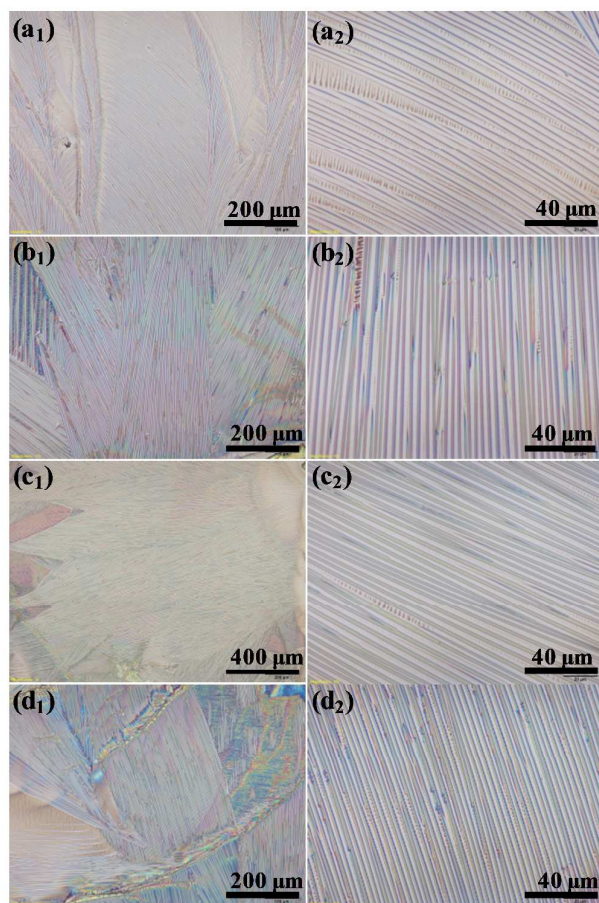


**Fig. 5** Optical microscope images of TCNQ microwire arrays formed with the substrate temperatures of (a<sub>1</sub>-a<sub>2</sub>) 25 °C, (b<sub>1</sub>-b<sub>2</sub>) 40 °C, (c<sub>1</sub>-c<sub>2</sub>) 70 °C, and (d<sub>1</sub>-d<sub>2</sub>) 100 °C, with solution concentration of 0.8 g/L.

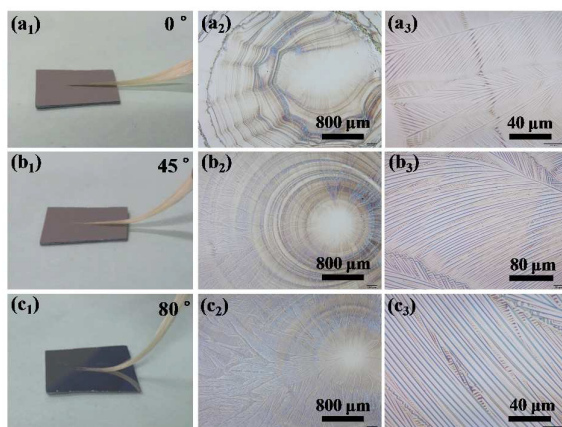


**Fig. 6** The effect of Inclination angles between the brush and the substrate on the growth of microwire array. (a<sub>1</sub>, a<sub>2</sub>, a<sub>3</sub>) 0°, (b<sub>1</sub>, b<sub>2</sub>, b<sub>3</sub>) 45°, (c<sub>1</sub>, c<sub>2</sub>, c<sub>3</sub>) 80°.

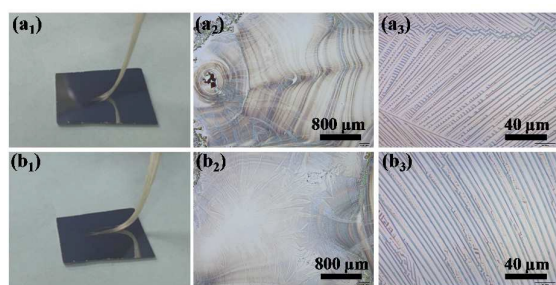


**Fig. 7** Pressure effect of the brush on growth of microwire array. (a<sub>1</sub>, a<sub>2</sub>, a<sub>3</sub>) Small pressure, (b<sub>1</sub>, b<sub>2</sub>, b<sub>3</sub>) Large pressure.

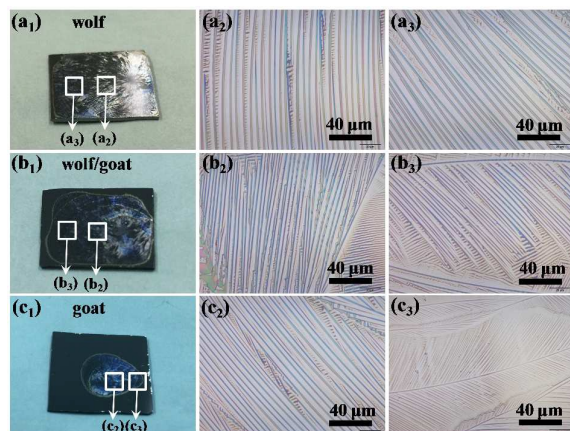


**Fig. 8** Effect of the type of the brush on the growth of microwire array. (a<sub>1</sub>, a<sub>2</sub>, a<sub>3</sub>) Wolf hair. (b<sub>1</sub>, b<sub>2</sub>, b<sub>3</sub>) Wolf/Goat hair. (c<sub>1</sub>, c<sub>2</sub>, c<sub>3</sub>) Goat hair.

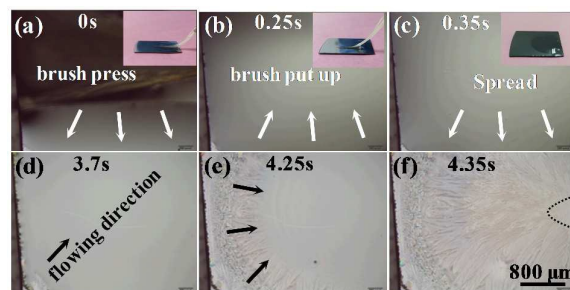


**Fig. 9** In situ time-resolved optical microscope images of the growth process of TCNQ microwire arrays. The insets in (a-c) are digital photographs corresponding to (a-c). The white arrows schematically show the flow direction of the solution. The dotted line shows the position of the head of a writing brush.

Based on the TCNQ microsheets and microwire arrays, the bottom-gate bottom-contact configuration field-effect transistors were fabricated in one step by brushing the solution on the pre-prepared electrode pattern, which provides a chance to investigate the anisotropic transport of TCNQ. Fig. 10a-c respectively show the schematic images of the devices and the corresponding transfer

curves for TCNQ microsheets and microwire arrays. The insets show the optical microscope images of the devices. According to the following formula:  $\mu = \frac{2L}{WC_i} \left( \frac{\partial \sqrt{I_{SD}}}{\partial V_G} \right)^2$  in the saturated regime, we calculated the mobility of devices.  $L$  and  $W$  are channel length and width, and  $C_i$  is capacitance per unit area of the insulator.

$C_i$  was calculated based on the SiO<sub>2</sub> as the dielectric with  $C_i = \frac{\epsilon_0 \epsilon_i}{d}$ , where  $\epsilon_0$  is the dielectric constant in vacuum,  $\epsilon_i$  is the relative dielectric constant, and  $d$  is the thickness of the dielectric. On the Si/SiO<sub>2</sub> substrate, the mobility of the TCNQ microwire arrays based transistor is  $1.8 \times 10^{-4} \text{ cm}^2 \text{ V}^{-1} \text{ s}^{-1}$ , which is nearly 2.5 times higher than that of the microsheel transistor. It is believed that the higher mobility in organic materials results from the stronger stacking interaction of adjacent molecules.<sup>32-33</sup> According to the crystal structure of TCNQ, TCNQ has the strongest molecular stacking direction in  $b$ -axis,<sup>21</sup> which provides the fastest crystal-growth direction resulting in the preferential growth of TCNQ in the direction of  $b$ -axis for the formation of the microwires. Therefore, the microwire with the orientation along the fastest crystal-growth direction is favorable to the carrier transport, which showing the potential of one-dimensional TCNQ microwires in electronic applications. It is found that the OTS modification on Si/SiO<sub>2</sub> substrate can further improve the mobility by one order of magnitude. As shown in Fig. 10c, the mobility of the TCNQ microwire arrays based transistor reaches  $1.83 \times 10^{-3} \text{ cm}^2 \text{ V}^{-1} \text{ s}^{-1}$  on the OTS modified Si/SiO<sub>2</sub> substrate. The OTS modification effectively decreases shallow traps density, and hence improves the mobility.<sup>34</sup> Our results are in good agreement with the previous reports. For example, Park et al. have reported that the field effect mobility of perylene organic thin film transistors (OTFT) increased over 100 times after OTS modification on SiO<sub>2</sub> dielectric.<sup>36</sup> To confirm the versatility of the procedure, we have prepared TIPS-pentacene microribbon arrays by a writing brush. The results are shown in supporting information. The mobility of TIPS-pentacene microribbon arrays can reach  $0.09 \text{ cm}^2 \text{ V}^{-1} \text{ s}^{-1}$ .

Based on TCNQ microwire arrays, the flexible field-effect transistors in bottom-gate top-contact configuration were fabricated

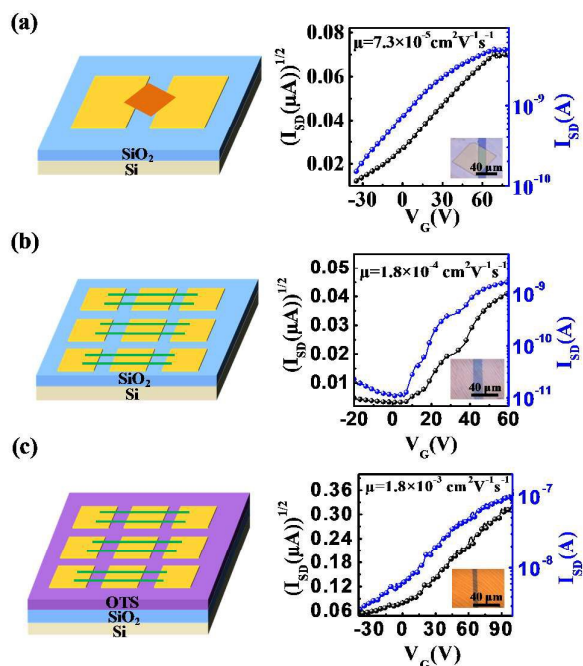


**Fig. 10** Schematic images of the TCNQ devices and the corresponding transfer curves measured in air at room temperature. (a) microsheet device on Si/SiO<sub>2</sub>, (b) microwire array device on Si/SiO<sub>2</sub>, (c) microwire array device on OTS modified Si/SiO<sub>2</sub>. The insets show the optical microscope images of the devices.

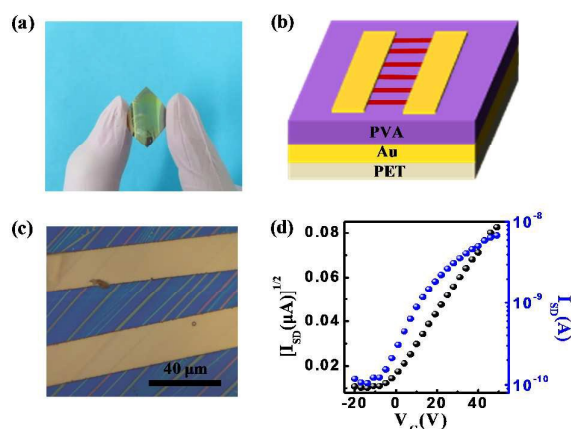


**Fig. 11** Flexible device based on TCNQ microwire arrays on PET substrate using PVA as dielectric. (a) Digital photograph of the device. (b) Schematic image of the device. (c) Optical microscope image of the device. (d) Transfer characteristic of a typical flexible device measured in air at room temperature.

on flexible PET substrate using PVA as dielectric by the “gold film stamping” method. Fig. 11a shows the digital photograph of the device on the bending PET substrate. The schematic image of the

flexible device is shown in Fig. 11b. Fig. 11c is the optical microscope image of a typical device. Fig. 11d is the transfer curve of the device, showing the mobility of  $1.7 \times 10^{-3} \text{ cm}^2 \text{ V}^{-1} \text{ s}^{-1}$ . The lower mobility on PVA dielectric than on OTS modified SiO<sub>2</sub> possibly originates from the hydroxy groups of PVA. Therefore this brush writing method also shows the promising potential in the fabrication of large-scale flexible devices and circuits.

## Conclusions

In conclusion, we have developed a novel solution-based assembly method based on a writing brush to yield highly-oriented, large-scaled and single-crystal TCNQ microwire arrays at success ratio as high as 93%. The large-scale microwire arrays can be grown onto the conventional substrates such as Si, Si/SiO<sub>2</sub> and glass, and unconventional substrates including flexible PET, curved glass hemisphere, and commercially available plastic contact lens. The brush hair induces the capillary force to change the flowing direction of the solution, causing a smaller solution concentration gradient and hence a larger-area single-crystal microwire arrays. The TCNQ microwire arrays are observed to be single crystals with a length extending up to millimeter level. And their preferential orientation is controlled perpendicular to the location direction of the brush hair. The coverage area of the microwire arrays with the consistent orientation can reach as large as  $1.5 \times 2.0 \text{ mm}^2$  at the optimized solution concentration (0.8 g/L) and substrate temperature (70°C). Compared with the conventional drop-casting method, our brush-writing process improves the success ratio for the formation of the microwire arrays. By increasing the concentration up to the near saturated solution (2.5 g/L), the large-scale regular uniform and high crystalline quality TCNQ microsheets with the size of 20-60 μm can be obtained. Both rigid and flexible devices can be easily realized in one step based on these microwire arrays and microsheets. The anisotropic transport of TCNQ crystals shows that the mobility of the TCNQ microwire array based transistor is nearly 2.5 times higher than that of the microsheet transistor, showing that the TCNQ microwire with the orientation along the fastest crystal-growth direction is favorable to the carrier transport. Such a low-cost and facile method may be used to fabricate the large-scale high-quality organic microwires, showing the potential in flexible and wearable electronics.

## Supporting information

The Supporting Information is available on the Nanoscale website.

## Acknowledgements

This work is supported by NSFC (61376074, 51273036, 51322305, 91233204, 61261130092, 61574032), Ministry of Science and Technology of China (2012CB933703), 111 Project (B13013), China Council Scholarship, and Fundamental Research Funds for the Central Universities (12SSXM001).



## Notes and references

- 1 H. T. Yi, M. M. Payne, J. E. Anthony and V. Podzorov, *Nat. Commun.*, 2012, **3**(1259).
- 2 I. Bae, S. K. Hwang, R. H. Kim, S. J. Kang and C. Park, *ACS Appl. Mater. Interfaces*, 2013, **5**(21), 10696-10704.
- 3 Y. Liu, X. Zhao, B. Cai, T. Pei, Y. Tong, Q. Tang and Y. Liu, *Nanoscale*, 2014, **6**(3), 1323-1328.
- 4 Y. Liu, Y. Han, X. Zhao, Y. Tong, Q. Tang and Y. Liu, *Synthetic Met.*, 2014, **198**, 248-254.
- 5 Y. Tong, Q. Tang, H. T. Lemke, K. M. Poulsen, F. Westerlund, P. Hammershoj, K. Bechgaard, W. Hu and T. Bjornholm, *Langmuir*, 2010, **26**(2), 1130-1136.
- 6 J. Jang, S. Nam, K. Im, J. Hur, S. N. Cha, J. Kim, H. B. Son, H. Suh, M. A. Loth, J. E. Anthony, J. J. Park, C. E. Park, J. M. Kim and K. Kim, *Adv. Funct. Mater.*, 2012, **22**(5), 1005-1014.
- 7 R. Bao, C. Zhang, X. Zhang, X. Ou, C. Lee, J. Jie and X. Zhang, *ACS Appl. Mater. Interfaces*, 2013, **5**(12), 5757-5762.
- 8 K. S. Park, B. Cho, J. Baek, J. K. Hwang, H. Lee and M. M. Sung, *Adv. Funct. Mater.*, 2013, **23**, 4776-4784.
- 9 Y. Su, X. Gao, J. Liu, R. Xing and Y. Han, *Phys. Chem. Chem. Phys.*, 2013, **15**(34), 14396-14404.
- 10 G. Giri, S. Park, M. Vosgueritchian, M. M. Shulaker and Z. Bao, *Adv. Mater.*, 2014, **26**(3), 487-493.
- 11 H. Li, C. Fan, M. Vosgueritchian, B. C. K. Tee and H. Chen, *J. Mater. Chem. C*, 2014, **2**(18), 3617-3624.
- 12 G. Lu, J. Chen, W. Xu, S. Li and X. Yang, *Adv. Funct. Mater.*, 2014, **24**(31), 4959-4968.
- 13 H. Zhao, D. Li, G. Dong, L. Duan, X. Liu and L. Wang, *Langmuir*, 2014, **30**(40), 12082-12088.
- 14 Y. Diao, B. C. K. Tee, G. Giri, J. Xu, D. H. Kim, H. A. Becerril, R. M. Stoltenberg, T. H. Lee, G. Xue, S. C. B. Mannsfeld and Z. Bao, *Nat. Mater.*, 2013, **12**(7), 665-671.
- 15 S. Y. Min, T. S. Kim, B. J. Kim, H. Cho, Y. Y. Noh, H. Yang, J. H. Cho and T. W. Lee, *Nat. Commun.*, 2013, **4**(1773).
- 16 A. Kumatani, C. Liu, Y. Li, P. Darmawan, K. Takimiya, T. Minari and K. Tsukagoshi, *Sci. Rep.*, 2012, **2**(393).
- 17 S. S. Lee, M. A. Loth, J. E. Anthony and Y. L. Loo, *J. Am. Chem. Soc.*, 2012, **134**(12), 5436-5439.
- 18 Y. Joo, G. J. Brady, M. S. Arnold and P. Gopalan, *Langmuir*, 2014, **30**(12), 3460-3466.
- 19 B. Mukherjee, *Indian J. Phys.*, 2014, **88**(10), 1073-1079.
- 20 L. L. Chua, J. Zaumseil, J. F. Chang, E. C. W. Ou, P. K. H. Ho, H. Sirringhaus and R. H. Friend, *Nature*, 2005, **434**, 194-199.
- 21 R. E. Long, R. A. Sparks and K. N. Trueblood, *Acta. Cryst.*, 1965, **18**, 932-939.
- 22 H. Jiang, X. Yang, Z. Cui, Y. Liu, H. Li and W. Hu, *Appl. Phys. Lett.*, 2009, **94**(12), 123308.
- 23 B. Mukherjee and M. Mukherjee, *Org. Electron.*, 2011, **12**(12), 1980-1987.
- 24 Q. Tang, Y. Tong, H. Li and W. Hu, *Appl. Phys. Lett.*, 2008, **92**(8), 083309.
- 25 T. A. Witten and L. M. Sander, *Phys. Rev. Lett.*, 1981, **47**(19), 1400-1403.
- 26 E. Menard, V. Podzorov, S. H. Hur, A. Gaur, M. E. Gershenson and J. A. Rogers, *Adv. Mater.*, 2004, **16**(23-24), 2097-2101.
- 27 M. Yamagishi, Y. Tominari, T. Uemura and J. Takeya, *Appl. Phys. Lett.*, 2009, **94**(5), 053305.
- 28 J. Yang, Y. Chen, X. Zhang, X. Ou and X. Zhang, *Nanotechnology*, 2011, **22**, 285606.
- 29 X. Zhao, T. Pei, B. Cai, S. Zhou, Q. Tang, Y. Tong, H. Tian, Y. Geng and Y. Liu, *J. Mater. Chem. C*, 2014, **2**(27), 5382-5388.
- 30 T. He, X. Zhang, J. Jia, Y. Li and X. Tao, *Adv. Mater.*, 2012, **24**(16), 2171-2175.
- 31 Y. Zhang, H. Dong, Q. Tang, Y. He and W. Hu, *J. Mater. Chem.*, 2010, **20**(33), 7029-7033.
- 32 L. Li, Q. Tang, H. Li, X. Yang, W. Hu, Y. Song, Z. Shuai, W. Xu, Y. Liu and D. Zhu, *Adv. Mater.*, 2007, **19**(18), 2613-2617.
- 33 J. L. Bredas, D. Beljonne, V. Coropceanu and J. Cornil, *Chem. Rev.*, 2004, **104**(11), 4971-5003.
- 34 K. Masatoshi and A. Yasuhiko, *J. Phys.: Condens. Matter*, 2008, **20**(184011).
- 35 D. Gundlach, Y. Lin, T. Jackson, S. Nelson and D. Schlom, *IEEE Electron Device Lett.*, 1997, **18**, 87-89.
- 36 D. Park, S. Kang, H. Kim, M. Jang, M. Noh, K.-H. Yoo, C. Whang, Y. Lee and M. Lee, *J. Vac. Sci. Technol. B*, 2005, **23**, 926.

We demonstrate a solution-based method by a writing brush to realize the controllable fabrication of highly-oriented and large-scale TCNQ microwire arrays which can be grown on the rigid and flexible substrates.

